supported by H.O. and T.K.; X.Z. performed the SAXS measurements; and N.T., T.K., K.A., H.O., Z.K. and H.T. contributed to writing the manuscripts and preparing the figures.

Additional information

Accession codes: The atomic coordinates and structure factors for IL-18, IL-18/IL-18Rα and IL-18/IL-18Rα/IL-18Rβ have been deposited in the RCSB Protein Data Bank under accession codes 3WO2, 3WO3 and 3WO4, respectively.

Supplementary Information accompanies this paper at http://www.nature.com/naturecommunications

Competing financial interests: The authors declare no competing financial interests.

Reprints and permission information is available online at http://npg.nature.com/reprintsandpermissions/

How to cite this article: Tsutsumi, N. *et al.* The structural basis for receptor recognition of human interleukin-18. *Nat. Commun.* 5:5340 doi: 10.1038/ncomms6340 (2014).

Molecular Immunology 58 (2014) 66–76

Contents lists available at ScienceDirect

Molecular Immunology

journal homepage: www.elsevier.com/locate/molimm

Functional assessment of the mutational effects of human *IRAK4* and *MyD88* genes

Takahiro Yamamoto[a,1], Naotaka Tsutsumi[b,1], Hidehito Tochio[b,**], Hidenori Ohnishi[a,*], Kazuo Kubota[a], Zenichiro Kato[a], Masahiro Shirakawa[b,c], Naomi Kondo[a,d]

[a] Department of Pediatrics, Graduate School of Medicine, Gifu University, 1-1 Yanagido, Gifu 501-1194, Japan
[b] Department of Molecular Engineering, Graduate School of Engineering, Kyoto University, Katsura, Nishikyo-ku, Kyoto 615-8510, Japan
[c] Core Research for Evolutional Science and Technology, Japan Science and Technology Corporation, 4-1-8 Hon-cho, Kawaguchi, Saitama 332-0012, Japan
[d] Heisei College of Health Sciences, 180 Kurono, Gifu 501-1131, Japan

ARTICLE INFO

Article history:
Received 3 October 2013
Received in revised form 8 November 2013
Accepted 9 November 2013
Available online 5 December 2013

Keywords:
IRAK4
MyD88
Myddosome
TIR domain
Death domain
Immune-deficiency

ABSTRACT

Human interleukin-1 receptor-associated kinase 4 (IRAK4) deficiency and myeloid differentiating factor 88 (MyD88) deficiency syndromes are two primary immune-deficiency disorders with innate immune defects. Although new genetic variations of *IRAK4* and *MyD88* have recently been deposited in the single nucleotide polymorphism (SNP) database, the clinical significance of these variants has not yet been established. Therefore, it is important to establish methods for assessing the association of each gene variation with human diseases. Because cell-based assays, western blotting and an NF-κB reporter gene assay, showed no difference in protein expression and NF-κB activity between R12C and wild-type IRAK4, we examined protein–protein interactions of purified recombinant IRAK4 and MyD88 proteins by analytical gel filtration and NMR titration. We found that the variant of IRAK4, R12C, as well as R20W, located in the death domain of IRAK4 and regarded as a SNP, caused a loss of interaction with MyD88. Our studies suggest that not only the loss of protein expression but also the defect of Myddosome formation could cause IRAK4 and MyD88 deficiency syndromes. Moreover a combination of *in vitro* functional assays is effective for confirming the pathogenicity of mutants found in IRAK4 and MyD88-deficiency patients.

1. Introduction

Interleukin-1 receptor-associated kinase (IRAK) 4 is the one of the essential molecules of the Toll/interleukin-1 receptor signaling pathway (Suzuki et al., 2002). In this pathway, ligand-induced hetero- or homodimerization of receptors recruits the Toll/interleukin-1 receptor homology domain (TIR domain) containing adaptor oligomers. One of these adaptors, MyD88, then binds IRAK4 (Burns et al., 2003). Recently, defects in the innate immune system have been shown to cause newly categorized human primary immune-deficiency syndromes (Al-Herz et al., 2011) such as human IRAK4 deficiency (Picard et al., 2003).

In affected IRAK4 deficient patients, invasive infections such as bacterial meningitis, sepsis, arthritis, or osteomyelitis are caused by *Streptococcus pneumonia*, *Staphylococcus aureus*, and *Pseudomonas aeruginosa* (Picard et al., 2010). Human MyD88 deficiency (von Bernuth et al., 2008) has remarkably similar clinical features to human IRAK4 deficiency. Interestingly, the life-threatening infections in IRAK4 or MyD88 deficient patients first occur during early infancy, but their frequency and severity reduce after the teenage years (Picard et al., 2011). Therefore, it is necessary for them to be diagnosed quickly.

IRAK4 and MyD88 proteins both consist of two major functional domains. In IRAK4, the death domain (DD) interacts with MyD88, while the kinase domain phosphorylates downstream signaling factors such as IRAK1, IRAK2, and subsequently causes activation of TNF Receptor Associated Factor 6 (TRAF6). In MyD88, both the DD and TIR domains interact in homotypic binding to similar domain structures. The domain–domain interactions are critical for these signaling pathways. IRAK4 and MyD88 form a hetero-oligomeric signaling complex via a shared DD, so-called Myddosome (Motshwene et al., 2009). Appropriate Myddosome

Abbreviations: DD, death domain; HEK, human embryonic kidney; ID, internal domain; IRAK, Interleukin-1 receptor-associated kinase; MyD88, myeloid differentiating factor 88; Mal, MyD88 adaptor-like; NMR, nuclear magnetic resonance; ELISA, enzyme-linked immunosorbent assay; TIR domain, Toll/interleukin-1 receptor homology domain; WT, wild type; SNP, single nucleotide polymorphism; IRAK4-DD, death domain of IRAK4; IRAK4-DD + ID, death domain and internal domain of IRAK4; MyD88-DD, death domain of MyD88; MyD88-DD + ID, death domain and internal domain of MyD88; MyD88-TIR, TIR domain of MyD88; Mal-TIR, TIR domain of Mal; TRAF, TNF receptor associated factor.

* Corresponding author. Tel.: +81 58 230 6386; fax: +81 58 230 6387.
** Corresponding author. Tel.: +81 75 383 2536; fax: +81 75 383 2541.
E-mail addresses: tochio@moleng.kyoto-u.ac.jp (H. Tochio), ohnishih@gifu-u.ac.jp (H. Ohnishi).
[1] Contributed equally as first authors.

0161-5890/$ – see front matter © 2013 Elsevier Ltd. All rights reserved.
http://dx.doi.org/10.1016/j.molimm.2013.11.008

formation can induce activation of the downstream signaling pathway, which eventually leads to the activation of NF-κB and activator protein 1 (AP-1).

Most previously identified causative mutations of human IRAK4 deficiency are nonsense or frame shift mutations that create early stop codons (Cardenes et al., 2006; Davidson et al., 2006; Enders et al., 2004; Krause et al., 2009; Ku et al., 2007; Medvedev et al., 2003; Picard et al., 2010; Takada et al., 2006; Yoshikawa et al., 2010), however, three missense mutations (M1V, R12C, and G298D) have been reported (Bouma et al., 2009; de Beaucoudrey et al., 2008; Hoarau et al., 2007). In human MyD88 deficiency, one nonsense mutation (E53X) and three missense mutations (E52del, L93P, and R196C) were reported as causative mutations (Conway et al., 2010; von Bernuth et al., 2008). Recently, new gene variations of *IRAK4* and *MyD88* have been deposited in the single nucleotide polymorphism (SNP) database following next-generation DNA sequencing, but the significance of these variants has not been evaluated. It is therefore important to establish methods to determine the association of gene variations with human diseases. For example, about MyD88, previous attempts have used western blotting, reporter gene assays, immunoprecipitation, and size exclusion chromatography of recombinant proteins to show that the SNPs MyD88 S34Y and R98C were loss-of-function variants (George et al., 2011), while another study used immunofluorescence to determine that S34Y fails to interact with IRAK4 (Nagpal et al., 2011).

Methods to detect the impaired responses to the Toll/interleukin-1 receptor agonists, such as enzyme-linked immunosorbent assay (ELISA) and flow-cytometry, are useful for rapid screening of innate immune deficiency syndromes (Davidson et al., 2006; Ohnishi et al., 2012a; Takada et al., 2006; von Bernuth et al., 2006). However, no *in vitro* method to assess the pathogenicity of novel variants of human *IRAK4*, *MyD88* and the other possible signaling components has been established. Therefore, when novel gene variants are found in that possible cases of IRAK4 or MyD88 deficiency syndromes, it is difficult to analyze the pathogenetic significance of these variants. In this study, we used a cell-based assay as well as *in vitro* protein-interaction analyses to show that IRAK4 R12C and R20W caused a loss of interaction with MyD88. This suggested that not only the loss of full-length IRAK4 and MyD88 protein expression but also the loss of Myddosome formation could cause IRAK4 and MyD88 deficiency syndromes.

2. Materials and methods

2.1. Cell culture

Human embryonic kidney (HEK) 293T cells were cultured in high glucose-containing DMEM (Invitrogen, Carlsbad, CA) supplemented with 10% heat-inactivated FBS (Sigma–Aldrich, St. Louis, MO), penicillin (100 U/ml), and streptomycin (100 μg/ml). Cells were incubated at 37 °C in a humidified atmosphere of 5% CO_2.

2.2. Vector preparations

cDNA encoding full-length IRAK4 (amino acid residues 1–460) or the DD and the internal domain (ID) of IRAK4 (IRAK4-DD + ID, amino acid residues 1–150) were tagged at the N terminus with a FLAG-epitope and cloned into the plasmid vector pcDNA3.1+ (Invitrogen). M1V was tagged at the C terminus because of a substitution of the start codon, and wild type (WT) tagged at the C terminus was prepared as a reference. Similarly, cDNA encoding full-length MyD88 (amino acid residues 1–296) or the TIR domain of MyD88 (MyD88-TIR, amino acid residues 148–296) tagged at the N terminus with a myc-epitope were cloned into the plasmid vector pcDNA3.1+ (Nada et al., 2012; Ohnishi et al., 2009). IRAK4 mutants and SNPs taken from dbSNP135 of the National Center for Biotechnology Information (NCBI, http://www.ncbi.nlm.nih.gov/snp) were generated using the GeneEditor *in vitro* Site-Directed Mutagenesis System (Promega, Fitchburg, WI). The pUNO hIL1R1(mb) vector (InvivoGen, San Diego, CA) was purchased and cDNA encoding IL-1RAcP and IL-18RAcPL were cloned into the plasmid vector pcDNA3.1+. The pGL4.32[luc2P/NF-κB-RE/Hygro] vector, used as an NF-κB luciferase reporter vector, and the pGL4.70[hRluc] vector, used as an internal control Renilla luciferase reporter vector, were purchased from Promega.

2.3. Western blot analysis

To detect protein expression, HEK293T cells were seeded on six-well plates at a density of 2×10^5/ml and transfected with 1 μg of expression plasmids of FLAG-tagged IRAK4 full length, FLAG-tagged IRAK4-DD, and myc-tagged MyD88 full length using Lipofectamine 2000 (Invitrogen) according to the manufacturer's instructions. After 48 h incubation, cells were harvested, washed with PBS, and lysed using CytoBuster Protein Extraction Reagent (Novagen, Darmstadt, Germany) containing a protease inhibitor mix (Roche Applied Science, Indianapolis, IN). All extracts were adjusted to contain equal amounts of total cellular proteins, as determined using the Bradford method. Supernatants and whole cell lysates were separated by electrophoresis on SDS polyacrylamide gels and transferred to nitrocellulose membranes using an iBlot Gel Transfer Device (Invitrogen). Membranes were blocked for 1 h in 5% BSA in TBST (pH 8.0, 10 mM Tris buffer containing 0.15 M NaCl and 0.1% Tween 20), then incubated at room temperature for 2 h with an anti-FLAG M2 monoclonal antibody (Sigma–Aldrich), anti-myc antibody (Invitrogen), or anti-β-actin antibody (Sigma–Aldrich) followed by incubation with anti-mouse IgG HRP conjugate (Promega) at room temperature for 30 min. Detection was performed using the ECL Chemiluminescent Substrate Reagent Kit (Invitrogen) and LightCapture system AE6970CP (ATTO, Tokyo, Japan).

2.4. NF-κB reporter gene activity

For the functional assessment of IRAK4, HEK293T cells, HEK293-hTLR1/2 cells (InvivoGen), HEK293-hTLR4-MD2-CD14 cells (InvivoGen) and HEK293-hTLR5 cells (InvivoGen) were transfected with NF-κB luciferase reporter vector, Renilla luciferase reporter vector, pcDNA3.1+ empty vector or pcDNA3.1+ FLAG-IRAK4 WT using Lipofectamine 2000. After transfection, cells were incubated for 24 h then stimulated with recombinant IL-1β (10 ng/ml) prepared as previously described (Wang et al., 2010), Pam3CSK4 (10 ng/ml, InvivoGen), LPS (10 ng/ml, Sigma–Aldrich), and recFLA-ST (10 ng/ml, InvivoGen) for 6 h. In a similar way, HEK293T cells were transfected as described above and with IL-18RAcPL, and stimulated with recombinant IL-18 (50 ng/ml) prepared as previously described (Kato et al., 2003; Li et al., 2003) for 6 h. Luciferase reporter gene activities were analyzed using the Dual-Luciferase Reporter Assay System (Promega). Similarly, HEK293T cells were transfected with pUNO-hIL1R1 vector, pcDNA3.1+ IL-1RAcP vector, NF-κB luciferase reporter vector, Renilla luciferase reporter vector, pcDNA3.1+ empty vector or pcDNA3.1+ FLAG-IRAK4 WT or variants, as described above. After transfection, cells were incubated for 24 h and luciferase reporter gene activities were analyzed.

For the functional assessment of MyD88, HEK293T cells were transfected with NF-κB luciferase reporter vector, Renilla luciferase reporter vector, and different amounts of pcDNA3.1+ myc-MyD88

WT or variants (5, 15 or 50 ng). The amounts of transfected plasmid were adjusted to an equal amount with pcDNA3.1+ empty vector. After transfection, cells were incubated for 24 h. To compare the dominant negative effect of MyD88, pcDNA3.1+ myc-MyD88-TIR WT or variants (5, 15 or 50 ng), pcDNA3.1+ IL-18RAcPL, NF-κB luciferase reporter vector, and Renilla luciferase reporter vector were co-transfected, and then, cells were incubated for 24 h and stimulated with/without IL-18 (10 ng/ml) for 6 h. Luciferase reporter gene activities were analyzed as described above.

The NF-κB activation of each condition was assessed in at least three independent experiments. The statistical significance of the differences in luciferase activities was determined using one-way ANOVA with Bonferroni's post-hoc test. The statistical significance was defined as $P < 0.05$.

2.5. Protein preparation

The portion of the human *IRAK4* gene encoding the DD + ID (amino acid residues 1–150) and the human *MyD88* gene encoding the DD and the ID (MyD88-DD + ID, amino acid residues 1–152) were cloned into vector pGEX-6P-1 (GE Healthcare, Little Chalfont, UK). These vectors were transformed into *Escherichia coli* BL-21 (DE3) (Novagen). IRAK4-DD + ID variants and MyD88-DD + ID, which were expressed as GST fusion proteins, were first purified by glutathione Sepharose 4B FF (GE Healthcare) affinity chromatography, and the GST-tag was removed by digestion with PreScission protease (GE Healthcare). Subsequently, the DD + IDs were purified by anion exchange chromatography (Q-Sepharose column; GE Healthcare) and gel filtration (Superdex 75 HR 26/60 column; GE Healthcare). Using a similar purification protocol, ^{1}H–^{15}N-labeled MyD88-DD + ID was prepared. All nuclear magnetic resonance (NMR) samples were uniformly ^{15}N-labeled and prepared in 210 μl solutions of H_2O/D_2O (95%/5%) containing 20 mM potassium phosphate buffer at pH 6.0 with 10 mM DTT. The portions of the human TIR domains of MyD88 WT and its mutants (M178I, R196C) and MyD88 adaptor-like (Mal) (Mal-TIR, amino acid residues 75–235) were cloned into pGEX-5X-1 and pGEX5X-3 vectors (GE Healthcare), respectively. The proteins were purified as previously described (Ohnishi et al., 2009).

2.6. Analytical gel filtration

Molecular masses of the purified recombinant proteins IRAK4-DD + ID and MyD88-DD + ID were evaluated by size exclusion chromatography. Gel filtration analysis was performed using a Superdex-200 10/300 GL column (GE Healthcare) attached to an AKTA purifier (GE Healthcare) at 10 °C. The column was equilibrated with 20 mM HEPES buffer (pH 7.0), 100 mM KCl, 10 mM DTT and 1 mM EDTA. The column was calibrated using a gel filtration standard kit (Bio-Rad, Hercules, CA). A total of 100 μl of 100 μM IRAK4-DD + ID and 100 μM MyD88-DD + ID proteins was applied to the gel filtration column. Protein elution was monitored by UV absorption at 280 nm. The molecular masses of these proteins were estimated using a calibration curve.

2.7. GST pull-down assays

GST-fusion proteins of MyD88-TIR and purified proteins of the TIR domain of Mal were incubated with Glutathione Sepharose 4B (GE Healthcare) in binding buffers (20 mM potassium phosphate buffer (pH 6.0), 0.1 mM EDTA, 10 mM DTT, and 0.2% Triton X-100) for 16 h. After four wash steps using 20 mM potassium phosphate buffer (pH 6.0), 100 mM KCl, 0.1 mM EDTA, 10 mM DTT, and 0.2% Triton X-100, the resin was analyzed by SDS-PAGE and Coomassie Brilliant Blue staining.

2.8. NMR titration

An aliquot of 0.25 equivalent amounts of non-labeled IRAK4 WT or its variants was added to 210 μl of 50 μM ^{15}N-labeled MyD88-DD + ID, with the exception for R20W, up to its 2.0 equivalent amounts. For the titration with R20W IRAK4-DD + ID, 25 μM MyD88-DD + ID was used. The samples were in 20 mM potassium phosphate (pH 6.0) and 10 mM DTT in H2O/D2O (95%/5%). At each titration point, 2D ^{1}H–^{15}N SOFAST-HMQC spectra were recorded at 298 K on Bruker Avance II 700 MHz spectrometer equipped with cryogenic probes. The 2D spectra were processed using NMRPipe (Delaglio et al., 1995) and analyzed using the Sparky (Goddard and Kneller, 1999) analysis software, whereas 1D projections were generated using Bruker TopSpin 3.1. A well-resolved NMR signal derived from a Trp sidechain aromatic ^{1}H–^{15}N pair in the projection was selected (supplementary Fig. S1B) at each titration point, and then intensities were normalized with the intensity of the corresponding NMR signal of ^{15}N MyD88-DD + ID recorded in the absence of IRAK4-DD + ID (Ohnishi et al., 2009). The normalized intensities were plotted as a function of the equivalent molar amounts of the titrant.

2.9. Protein stability assay

HEK293T cells were seeded on six-well plates at a density of 2×10^5/ml and transfected with 1 μg of expression plasmids Flag-tagged IRAK4-DD using Lipofectamine 2000. After 48 h, cells were treated with 25 μM cycloheximide for 0, 24, 48, and 72 h (Fukao et al., 1999). Cellular extracts were prepared in CytoBuster Protein Extraction Reagent containing complete protease inhibitor mix. All extracts were adjusted to contain equal amounts of total cellular proteins, as determined using the Bradford method. Western blot analysis with anti-FLAG antibody was carried out using standard protocols as described above.

3. Results

3.1. Cell-based assays of IRAK4 variants

3.1.1. Protein expression of IRAK4

To functionally characterize the genetic variants of *IRAK4*, FLAG-tagged full-length expression constructs corresponding to the loss-of-function mutations that were previously reported as pathogenic mutations ('*IRAK4* mutants') and nonsynonymous SNPs ('*IRAK4* SNPs') were generated. In this study, we selected the six IRAK4 mutants (M1V, a missense mutation of start codon reported in Slovenia (de Beaucoudrey et al., 2008); R12C, a missense mutation reported in France and located in the DD (Hoarau et al., 2007); c.118insA and R183X, mutations reported in Japan that include a frame shift mutation (Picard et al., 2010; Takada et al., 2006); Q293X, the most common mutation in Europe (Picard et al., 2010); G298D, a missense mutation reported in UK and located in the kinase domain (Bouma et al., 2009)) and five SNPs in the DD (Fig. 1A). Our five SNPs were all within the DD as we focused on the interaction between IRAK4 and MyD88.

No protein expression could be detected of the three *IRAK4* mutations M1V, Q293X, and c.118insA. R183X expressed a smaller protein than WT, while G298D protein expression levels were decreased (Fig. 1B). The expression of R12C was comparable with WT as were expression levels of all SNPs (Fig. 1C).

3.1.2. Inhibition of NF-κB activation of IRAK4

Next, *IRAK4* variants were tested for NF-κB reporter gene activity using a dual luciferase assay system. As Medvedev et al.

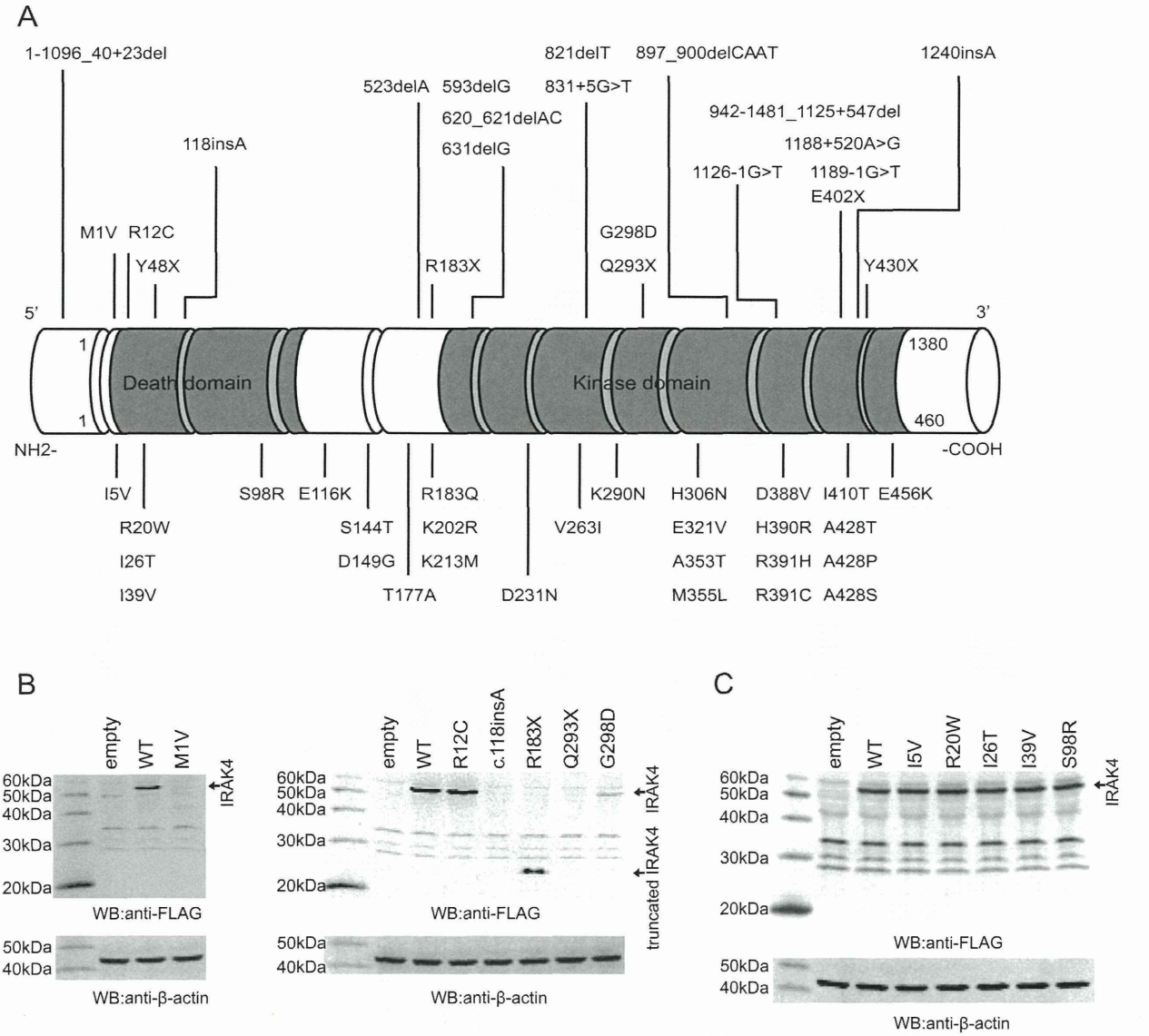

Fig. 1. Protein expression of *IRAK4* variants. (A) Schematic representation of *IRAK4* showing all identified mutations and nonsynonymous SNPs. *IRAK4* consists of 12 exons and the protein is composed of an N-terminal death domain and C-terminal kinase domain. Mutations are annotated at the upper side of this schema, and SNPs at the lower. (B) Expression levels of *IRAK4* mutants in HEK293T cells. Protein expression of M1V, Q293X, and c.118insA could not be detected. R183X expressed a truncated protein and the expression level of G298D was low. (C) Expression levels of *IRAK4* SNPs in HEK293T cells. All SNPs examined in this study expressed protein at the same level as WT.

(2003) previously reported that IL-1β-induced NF-κB activation was inhibited by overexpressed IRAK4 in HEK293T cells, we repeated their method with five different HEK293 cell lines and their appropriate ligands to compare the inhibition of NF-κB activation (Fig. 2). IL-1β, IL-18 and the ligands of TLR1/2, TLR4, and TLR5-induced NF-κB activations were not significantly inhibited by overexpressed IRAK4 (Fig. 2A–E), but the NF-κB activity enhanced by both transiently transfected IL-1R1 and IL-1RAcP could be significantly inhibited by overexpressed IRAK4 (Fig. 2F).

This system was used to compare *IRAK4* variants. Fig. 2G shows that NF-κB activation of the mutants c.118insA, R183X, Q293X, and G298D was less inhibited than WT. However, R12C showed a similar activity level to WT, although this mutation was previously reported to be a loss-of-function mutant in a human IRAK4 deficiency patient (Hoarau et al., 2007). Fig. 2H shows that all *IRAK4* SNPs significantly inhibited NF-κB activity to the same extent as WT. Only R20W showed a stronger inhibitory effect.

3.2. Cell-based assays of MyD88 variants

3.2.1. Protein expression of MyD88

We analyzed four previously reported loss-of-function mutations of MyD88: E52del, E53X, and L93P located in the DD, and R196C located in the TIR domain, as well as three SNPs: S34Y and R98C (loss-of-function variants (George et al., 2011; Nagpal et al., 2011) located in the DD, and M178I in the TIR domain (Fig. 3A). To functionally characterize the *MyD88* genetic variants, myc-tagged full-length expression constructs corresponding to the loss-of-function mutations ('*MyD88* mutants') and nonsynonymous SNPs ('*MyD88* SNPs') were generated. No protein expression was detected of S34Y and E53X, while expression of E52del and L93P was very low. On the other hand, expression levels of R98C, M178I, and R196C were similar to WT (Fig. 3B).

3.2.2. NF-κB activity of MyD88

Next, we assessed the abilities of *MyD88* variants to activate the NF-κB signaling pathway using a dual luciferase assay system in

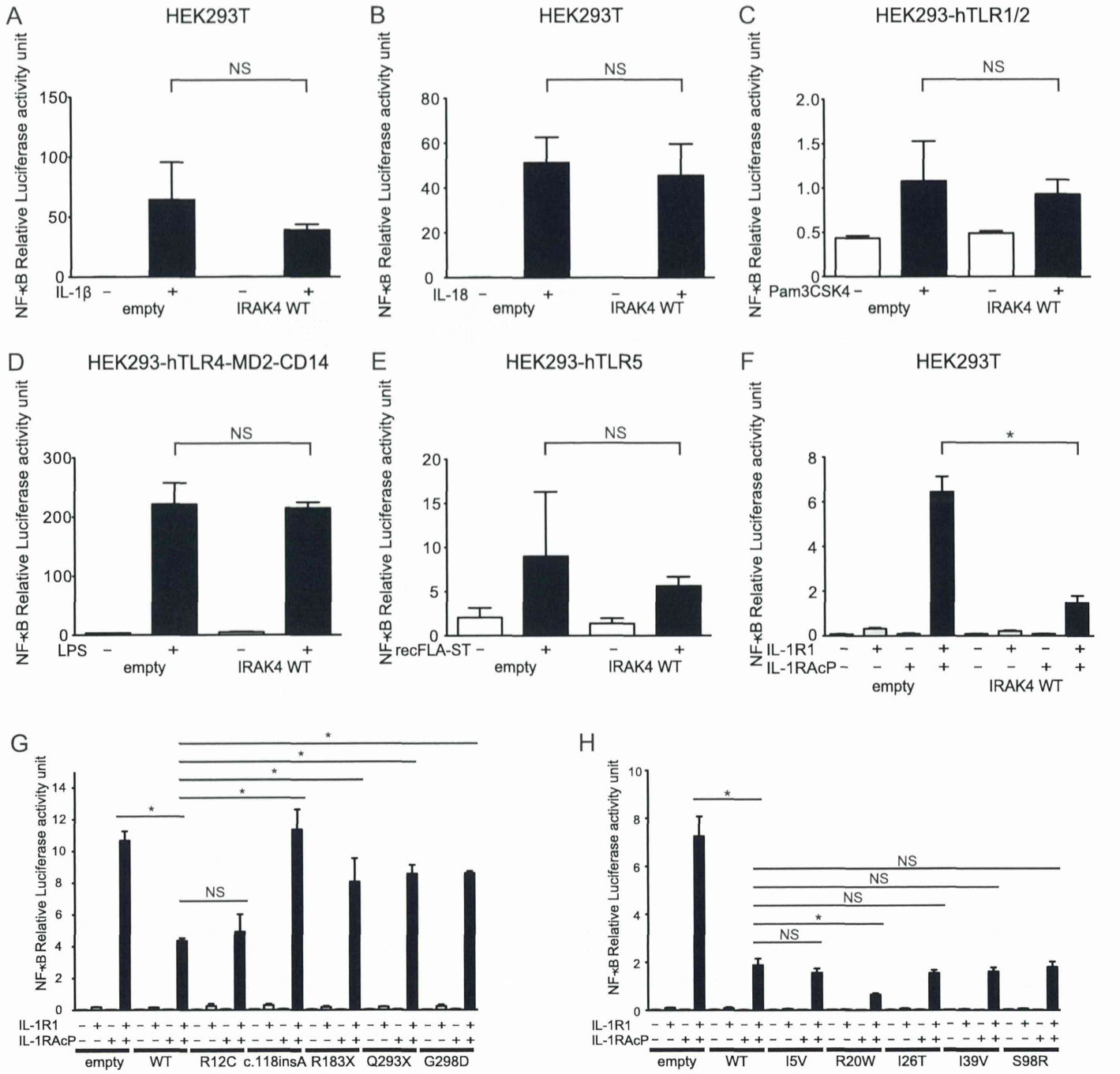

Fig. 2. Cell-based NF-κB activity assays of *IRAK4* variants. (A-F) The inhibition of NF-κB activation in five different cell lines by IRAK4. IL-1β- (10 ng/ml), IL-18- (50 ng/ml), Pam3CSK4- (10 ng/ml), LPS- (10 ng/ml) and recFLA-ST- (10 ng/ml) induced NF-κB activations was not significantly inhibited by overexpressed IRAK4 WT in HEK293T cells (A, B, F), HEK293-hTLR1/2 cells (C), HEK293-hTLR4-MD2-CD14 cells (D), and HEK293-hTLR5 cells (E). Transient transfection of both IL-1R1 and IL-1RAcP significantly enhanced NF-κB activity in HEK293T cells, which could be significantly inhibited by overexpressed IRAK4. (G and H) The inhibition of NF-κB activation by *IRAK4* variants in HEK293T cells. The inhibition by mutants c.118insA, R183X, Q293X, and G298D of NF-κB activation induced by co-transfection both IL-1R1 and IL-1RAcP was significantly less than in WT. R12C showed a similar inhibition level to WT. All *IRAK4* SNPs significantly inhibited NF-κB activity as well as WT. Only R20W showed a stronger inhibition of NF-κB activity than WT. Data represent the mean ± SD of a representative experiment ($n = 3$). Asterisk indicates a statistically significant difference between WT and the others. NS means "not-significant".

HEK293T cells. Fig. 3C shows that overexpression of S34Y, E52del, E53X, L93P, R98C, and R196C resulted in lower NF-κB activation than that of WT. We previously reported that the truncated MyD88 lacking a DD (MyD88-TIR) inhibited IL-18-stimulated NF-κB activation by means of a dominant negative effect (Ohnishi et al., 2012b). Therefore, in the present study, we examined NF-κB activation inhibition from a dominant-negative effect in HEK293T cells transiently co-transfected with IL-18RAcP and MyD88-TIR WT, or M178I and R196C (Fig. 3D). MyD88-TIR M178I inhibited NF-κB activation to a similar level as WT, but MyD88-TIR R196C was compromised in its effect to inhibit NF-κB activation.

3.3. GST pull-down assay of MyD88-TIR to Mal-TIR

MyD88 interacts with Mal via a shared TIR domain and activates a downstream signaling pathway. To analyze the mutations

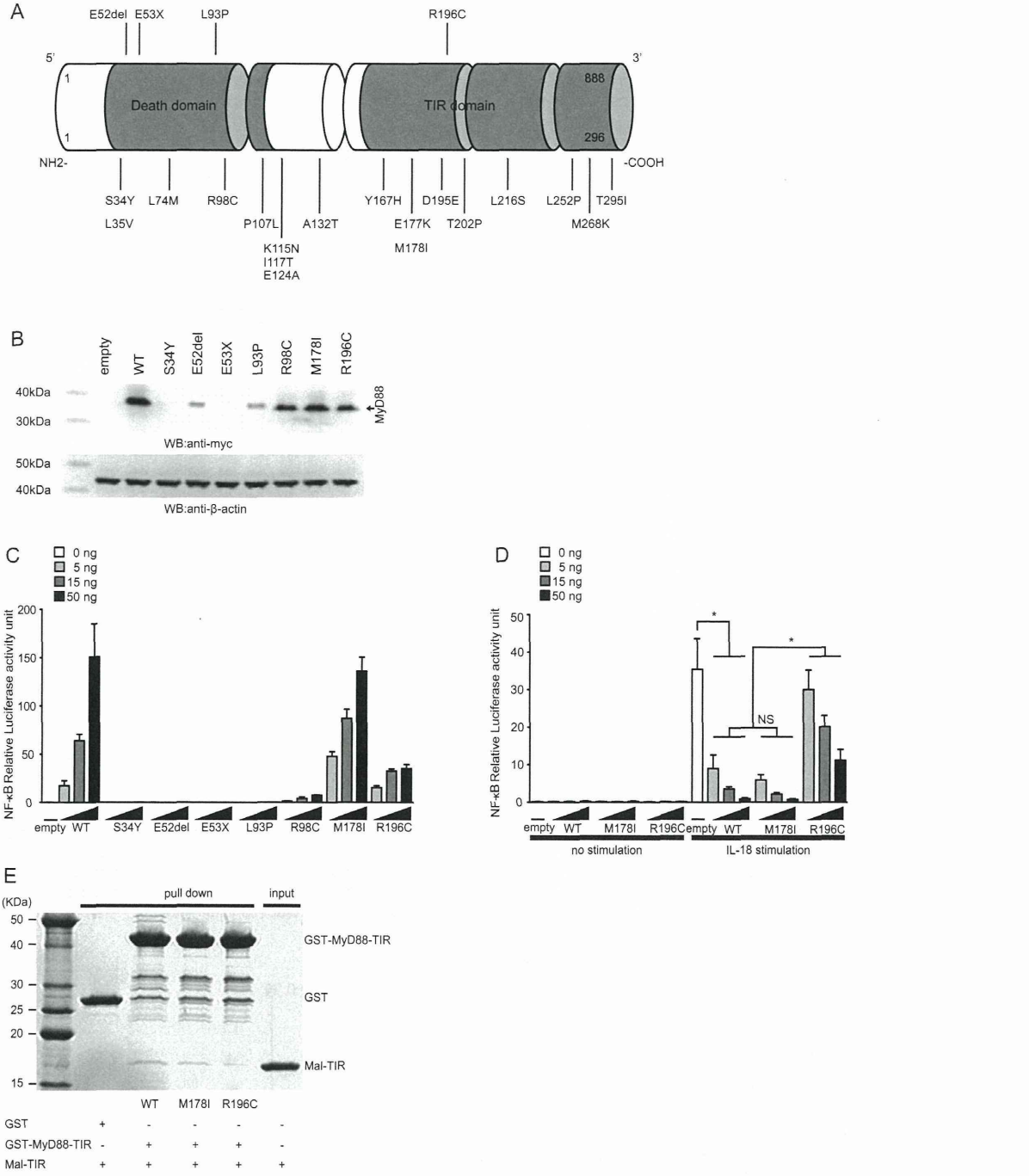

Fig. 3. Cell-based assays of *MyD88* variants. (A) Schematic representation of *MyD88* with all identified mutations and nonsynonymous SNPs. *MyD88* consists of five exons and the protein is composed of an N terminal death domain and C-terminal TIR domain. Mutations are annotated at the upper side of this schema, and SNPs at the lower. (B) Expression levels of *MyD88* variants in HEK293T cells. The protein expression of S34Y and E53X could not be detected, and that of E52del and L93P was very low. The expression levels of R98C, M178I, and R196C were similar to that of WT. (C) NF-κB reporter gene activities of *MyD88* variants in HEK293T cells. S34Y, E52del, E53X, L93P, R98C, and R196C were compromised in the ability to enhance NF-κB activation, with the exception of M178I. (D) Dominant negative inhibitory effects of MyD88-TIR variants in HEK293T cells. MyD88-TIR R196C failed to inhibit NF-κB activation. Data represent the mean ± SD of a representative experiment ($n = 3$). All data were compared at each transfection dose. Asterisk indicates statistically significant difference between WT and the others. NS means "not-significant". (E) Binding assays for WT or mutant MyD88-TIRs with Mal-TIR using GST pull-down assays. M178I interacted with Mal-TIR as well as WT. R196C showed a reduced interaction with Mal-TIR.

located in the TIR domain of MyD88, we carried out a GST pull-down assay of MyD88-TIR and Mal-TIR (Fig. 3E). As we reported previously (Nada et al., 2012; Ohnishi et al., 2009), MyD88-TIR R196C showed a significant decrease in its ability to directly bind to Mal-TIR, while MyD88-TIR M178I interacted with Mal-TIR as well as WT.

3.4. Analytical gel filtration of IRAK4 and MyD88

To compare the interaction between MyD88 and IRAK4, analytical gel filtration was carried out. We purified MyD88-DD + IDs and IRAK4-DD + IDs recombinant proteins, and analyzed the elution profiles of mixtures of MyD88 WT or mutants in the presence

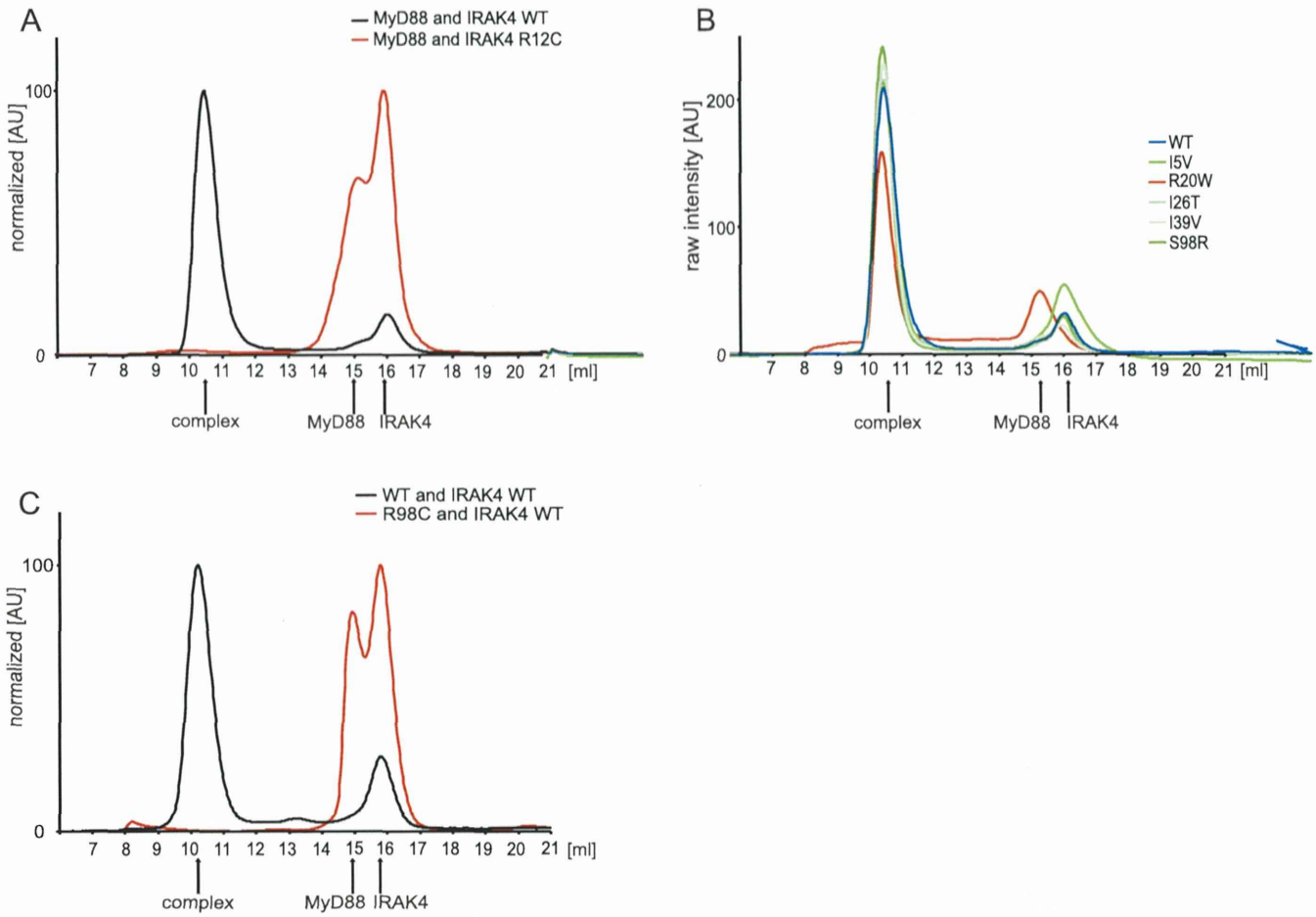

Fig. 4. Analytical gel filtration of IRAK4 and MyD88. (A) IRAK4-R12C failed to interact with MyD88. R12C was unable to assemble into a Myddosome as shown by size exclusion chromatography of mixtures of bacterially purified MyD88-DD + IDs and IRAK4-DD + IDs (added in excess). MyD88-DD + ID WT + IRAK4-DD + ID WT mixture eluted in a discrete complex peak that was absent from R12C mixtures. (B) IRAK4 SNPs interacted with MyD88 WT. Only IRAK4 R20W showed a decreased peak intensity of complete complex and residual peak of MyD88-DD + ID despite mixing an excess of IRAK4. (C) MyD88-R98C failed to interact with IRAK4. Individual peak fractions from gel filtration, purified MyD88-DD + ID or IRAK4-DD + ID alone (for size comparison) were analyzed by reducing SDS-PAGE (data not shown).

of a molar excess of IRAK4-DD + ID WT or mutants. Individual fractions or purified reference proteins were analyzed by SDS-PAGE (data not shown). The estimated molecular weights were calculated using a calibration curve, and were 30.6 kDa, 48.3 kDa, and 423 kDa for IRAK4-DD + ID, MyD88-DD + ID, and their complex, respectively. Although IRAK4-DD was eluted as a 1mer (George et al., 2011; Lin et al., 2010; Motshwene et al., 2009), IRAK4-DD + ID was mainly eluted as a 2mer. While MyD88 was mainly eluted as a 3mer. IRAK4 WT formed a characteristic oligomer by mixing with MyD88 WT, but not R98C, as previously reported (Fig. 4C) (Nagpal et al., 2011). Moreover, IRAK4 R12C also failed to form a complex (Fig. 4A). By contrast, *IRAK4* SNPs interacted with MyD88 WT (Fig. 4B), but only IRAK4 R20W showed a decreased intensity of the complex and residual peak of MyD88-DD + ID, despite an excess amount of IRAK4.

3.5. NMR titration

The IRAK4–MyD88 interaction was also examined using NMR spectroscopy for which 2D ^{1}H–^{15}N correlation NMR spectra of ^{15}N-labeled MyD88-DD + ID were recorded in the presence or absence of various concentrations of IRAK4-DD + ID or its derivatives. Changes of NMR signal intensities of a Trp residue in ^{15}N-labeled MyD88-DD + ID following titration were used to monitor the interaction (Fig. 5). The normalized NMR signal intensity steeply decreased upon IRAK4 titration. Attenuation of the NMR signal could be

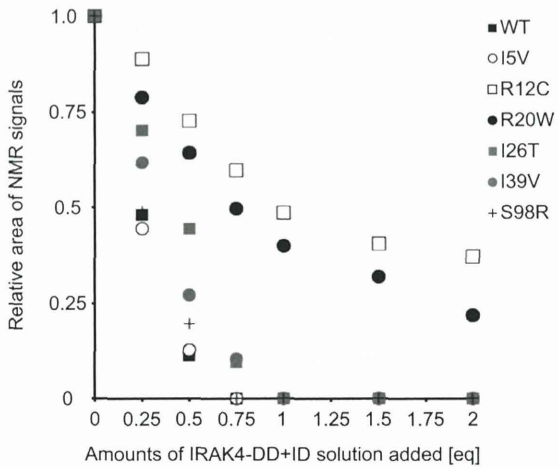

Fig. 5. NMR titration study of ^{1}H–^{15}N-MyD88-DD + ID and IRAK4-DD + ID. Normalized intensities of NMR signals, obtained from the NMR titration experiment (Supplemental Fig. S1), were plotted in a function of equivalent moles (eq) of IRAK4-DD + ID added to ^{15}N-MyD88-DD + ID. The attenuation of signal intensities was presumably caused by formation of complexes between MyD88-DD + ID and IRAK4-DD + ID. NMR signal attenuation of R12C and R20W was significantly suppressed relative to WT, indicating a weak affinity for MyD88-DD + ID. Black box, white circle, white box, black circle, gray box, gray circle, and black cross indicate the normalized intensities of WT, I5V, R12C, R20W, I26T, I39V, and S98R, respectively.

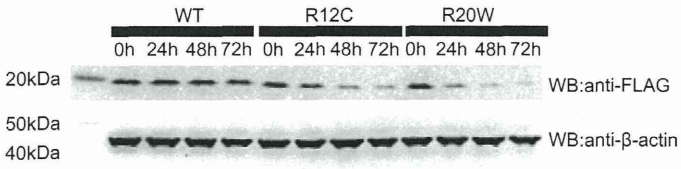

Fig. 6. Stability of IRAK4-DD variants in HEK293T cells. Cells were incubated in cycloheximide (25 μM) for the indicated times before preparation of cell extracts for SDS-PAGE separation and immunoblotting with an anti-FLAG antibody. IRAK4-DD WT maintained a steady state of protein structure, but R20W began to collapse after 24 h.

interpreted as a result of the formation of large protein complexes involving ^{15}N-labeled MyD88-DD + ID, indicating an interaction of the titrated IRAK4-DD + ID with ^{15}N-MyD88-DD + ID. Four IRAK4 derivatives, I5V, I26T, I39V, and S98R, showed a similar attenuation pattern to that of WT. By contrast, attenuation of NMR signal intensities was significantly suppressed when one of two derivatives, R12C or R20W, was used as a titrant. These observations suggest that the affinity of R12C and R20W towards MyD88-DD + ID was weaker than that of WT.

3.6. Instability of IRAK4 R12C and R20W

In the analytical gel filtration and NMR titration assays, IRAK4 R12C failed to interact with MyD88. On the other hand, IRAK4 R20W could interact with MyD88, but the amount of complete complex was lower than WT and other SNPs. Additionally, R12C and R20W were predicted to be "probably damaging" with scores of 1.000 and 0.998, respectively, by the PolyPhen-2 algorithm (http://genetics.bwh.harvard.edu/pph2/) (Adzhubei et al., 2010). Therefore, we next evaluated the protein stability of IRAK4-DD + ID R12C and R20W compared with WT following treatment with cycloheximide (Fig. 6). IRAK4-DD + ID WT protein levels did not change during 72 h of cycloheximide treatment, but R12C protein levels slightly decreased after 48 h of treatment, and R20W protein levels decreased after 24 h of treatment.

4. Discussion

4.1. In vitro assays for assessments of the mutational effects of human IRAK4 gene

Several cell-based functional assays of *IRAK4* mutants have previously been described, but the mutational effects of novel mutations have not been confirmed. For example, Lye et al. examined the NF-κB activation of *IRAK4* mutants using IRAK4-knocked out murine fibroblasts (Lye et al., 2004), while Qin et al. (2004) used human fibroblasts derived from an IRAK4 deficiency patient. Medvedev et al. (2005) examined the IL-1 signaling complex formation of an *IRAK4* mutant using immunoprecipitation. In the present study, we examined selected *IRAK4* mutations, including three previously reported missense mutations (Fig. 1A). Protein expression levels of WT and R12C were similar (Fig. 1B), so we then assessed the signaling function using HEK293T cells (Medvedev et al., 2003) as it is difficult to obtain an IRAK4-deficient human cell line. IRAK4 Q293X protein expression was undetectable and it did not appear to inhibit NF-κB activity (Figs. 1B and 2G), which agrees with the results of Medvedev et al. (2003).

The other *IRAK4* mutants, with the exception of R12C which expressed undetectable or low level IRAK4 protein, also did not inhibit NF-κB activity. On the other hand, R12C inhibited NF-κB activity to almost the same extent as WT. This suggests that overexpressed IRAK4 protein only inhibits NF-κB activity when full-length IRAK4 is expressed at levels above a certain threshold. All SNPs analyzed expressed similar protein levels and inhibited NF-κB activity to the same level as WT (Fig. 1C and E). Interestingly, R20W showed a significantly stronger inhibition of NF-κB activity than WT and other SNPs, while the PolyPhen-2 algorithm "probably damaging" prediction for R12C and R20W meant that the behavior of both was uncertain.

To clarify this, we focused on these two variants. From information about the Myddosome protein structure (PDB code: 3MOP) (Lin et al., 2010), residues R12 and R20 appeared to be located on the surface of IRAK4-DD, in the interface between IRAK4 and MyD88, and to directly interact with MyD88-DD E102 and D46, respectively (Fig. 7B). A protein–protein interaction study was used to assess the mutational effect of these residues. MyD88-DD R98 was located in the interface to IRAK4-DD (George et al., 2011), while MyD88-TIR R196 was located in the interface to Mal-TIR (Ohnishi et al., 2009). These arginine to cysteine substitutions caused a change in protein–protein interaction abilities. The recombinant proteins of IRAK4-DD + ID WT and MyD88-DD + ID WT formed a higher order oligomeric complex, but IRAK4 R12C failed to interact with MyD88.

While we were preparing this manuscript, T77del, a novel mutation of human IRAK4 deficiency, was reported as a loss-of-expression variant following a western blot of a patient's fibroblasts (Andres et al., 2013). Lin et al. (2010) used immunoprecipitation to show that both T76 and N78 are critical residues for the interaction with MyD88. Therefore T77 might be critical not only for protein expression but also the interaction with MyD88. It should be noted that although IRAK4 S98 is located on the surface of IRAK4-DD (Fig. 7A), it is distant from the interface with MyD88-DD. From the complex structural information, S98 might be located in the interface between IRAK4 and IRAK2. Future work should carry out a protein interaction study between IRAK4 S98R and IRAK2 or IRAK1 to evaluate the pathogenicity of IRAK4 S98R.

All *IRAK4* SNPs examined in the present study formed a complex in analytical gel filtration. Interestingly, R20W also formed a complex, albeit less than WT and the other SNPs. In addition, an incomplete complex of IRAK4 R20W and MyD88 was observed between the peak of unbound proteins and complete complex (Fig. 4B). Moreover, the NMR signal attenuation titrated with IRAK4 R12C and R20W was reduced compared with WT (Fig. 5), suggesting that the interaction was weakened by amino acid substitutions. From these results, we speculated that not only the mild loss of protein–protein interaction, but also the loss of IRAK4-DD R20W protein stability inhibits the formation of a complete complex of IRAK4 and MyD88. Therefore, we examined protein stability using cycloheximide. The stability of IRAK4-DD R12C was slightly lower, but that of R20W was much lower than WT and R12C (Fig. 6). Thus it is conceivable that the hydrophilic Arg20 substitution to hydrophobic tryptophan reduces the stability of the protein structure. Finally, we propose the possibility that not only IRAK4 R12C but also R20W has an impact on human IRAK4 deficiency (Table 1).

4.2. In vitro assays for assessments of the mutational effects of human MyD88 gene

Recently, the loss-of-function variants S34Y and R98C were found in naturally occurring *MyD88* SNPs (George et al., 2011; Nagpal et al., 2011). The functions of these variants were also shown by a luciferase reporter gene assay in HEK293 I3A cells, and interaction analysis with recombinant proteins. On the other hand, Napgal et al. carried out an initial functional assay of *MyD88* variants using a luciferase reporter gene assay in HEK293T cells, which are not MyD88-deficient. In addition, Loiarro et al. (2009) used immunoprecipitation in HEK293T cells to indicate that E52 and Y58 were key residues that interact with both IRAK1 and IRAK4, and that K95 was an important residue to interact with IRAK4. In this

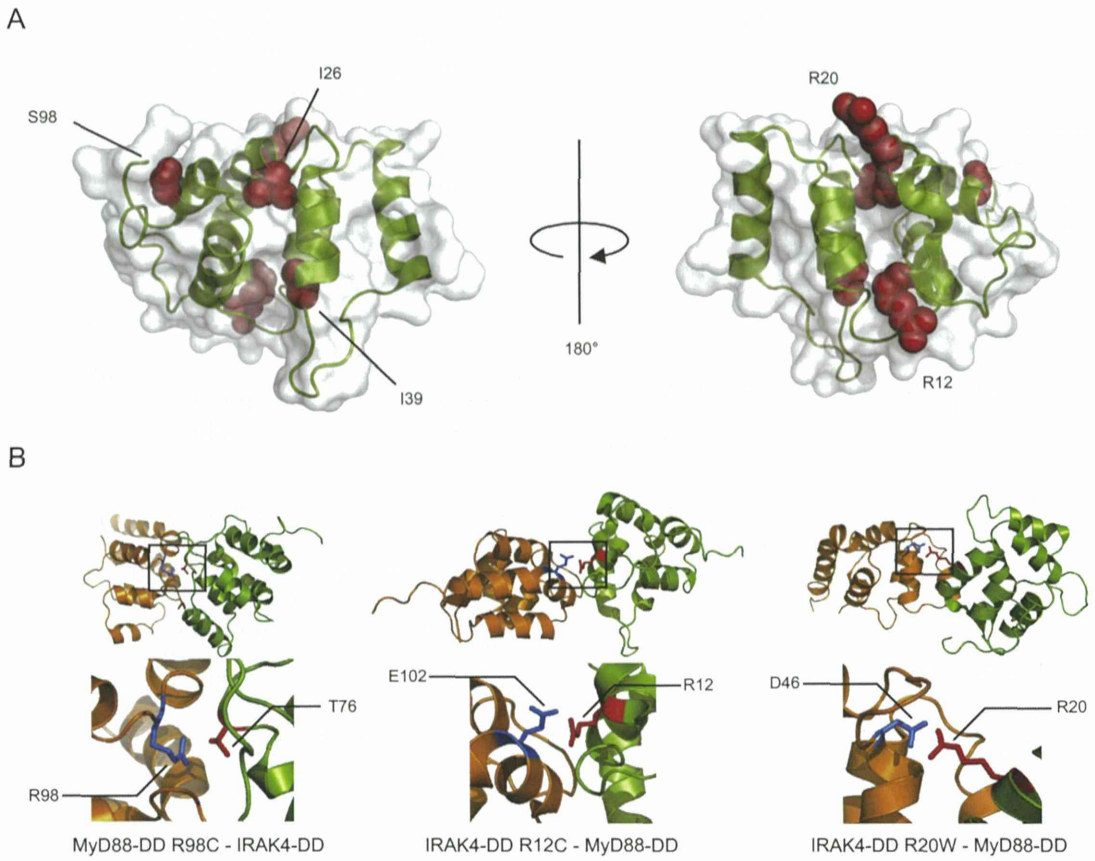

Fig. 7. Protein structure of IRAK4-DD. (A) Schematic representation of IRAK4-DD (Protein Data Bank accession code 2A9I) generated with PyMOL (DeLano Scientific, www.pymol.org). Mutants and variants are shown as red full-surface amino acid residues. R12, R20, and S98 are located on the surface of IRAK4-DD. (B) 3D interaction models of IRAK4-DD (green) with MyD88-DD (orange). MyD88-DD R98 (side chain shown as a blue stick) interacts with IRAK4-DD T76. IRAK4-DD R12 and R20 (side chains shown as red sticks) interact with MyD88-DD E102 and D46, respectively.

study, we revealed decreased protein expression levels of *MyD88* variants (S34Y, E52del, and L93P) with HEK293T cells, indicating that they have unstable protein structures (Fig. 3B). Moreover, R98C as well as the loss-of-expression variants had lower NF-κB activity than MyD88 WT (Fig. 3C), while MyD88-DD R98C had an impaired direct interaction with IRAK4-DD WT (Fig. 4C). Consequently, MyD88 R98C can be a risk-allele for MyD88 deficiency, because it showed similar to IRAK4 R12C about the results of interaction assay between MyD88-DD and IRAK4-DD. Thus, the results of MyD88-DD gene variation from a cell-based assay using a MyD88-non-deficient cell line are consistent with the protein interaction study, unlike the *IRAK4* variants.

MyD88 interacts with Mal via a shared TIR domain. We previously found that MyD88-TIR R196C had stable protein folding but a significant decrease in its ability to directly bind Mal-TIR (Nada et al., 2012; Ohnishi et al., 2009). TIR domains have an important functional region, the BB loop, which interacts with other TIR domain-containing proteins. As the R196C mutation and M178I SNP are located in or near the BB loop of the MyD88 TIR domain, we tested MyD88 full-length-induced NF-κB activation and the inhibition of ligand-induced NF-κB activity caused by a dominant-negative effect to assess the functional effect of M178I. MyD88 full-length M178I significantly enhanced NF-κB activity, as seen in WT (Fig. 3C). MyD88-TIR M178I inhibited NF-κB activation to the same extent as WT, but R196C did not (Fig. 3D). Furthermore, a GST pull-down assay using recombinant purified proteins found that MyD88-TIR M178I interacted with Mal-TIR as well as WT (Fig. 3E), which was consistent with the cell-based assays. Therefore we determined M178I to be a variant, although the mutation of a neighboring residue, I179N also called the Poc

Table 1
Summary of the expression and functional analysis of *IRAK4* variants.

Gene	Variant	Protein expression	NF-κB activity	Interaction	Protein stability	Pathogenicity
IRAK4	M1V	Absent	–	–	–	Reported
	I5V	Normal	Inhibited	Normal	–	Polymorphism
	R12C	Normal	Inhibited	Reduced	Mild reduced	Reported
	R20W	Normal	Inhibited	Mild reduced	Reduced	Probable
	I26T	Normal	Inhibited	Normal	–	Polymorphism
	I39V	Normal	Inhibited	Normal	–	Polymorphism
	c.118insA	Severely reduced	Not inhibited	–	–	Reported
	S98R	Normal	Inhibited	Normal	–	Polymorphism
	R183X	Truncated	Not inhibited	–	–	Reported
	Q293X	Severely reduced	Not inhibited	–	–	Reported
	G298D	Reduced	Not inhibited	–	–	Reported